



Collateral-Core Ratio as a Novel Predictor of Clinical Outcomes in Acute Ischemic Stroke

Jinhao Lyu¹ · Sa Xiao^{2,3} · Zhihua Meng⁴ · Xiaoyan Wu⁵ · Wen Chen⁶ · Guohua Wang⁷ · Qingliang Niu⁸ · Xin Li⁹ · Yitong Bian¹⁰ · Dan Han¹¹ · Weiting Guo¹² · Shuai Yang¹³ · Xiangbing Bian¹ · Qi Duan¹ · Yina Lan¹ · Liuxian Wang¹ · Tingyang Zhang¹ · Caohui Duan¹ · Ling Chen¹⁴ · Chenglin Tian¹⁵ · Yuesong Pan^{16,17} · Xin Zhou² · Xin Lou¹ · on behalf of the MR-STARS Investigators

Received: 16 March 2022 / Revised: 26 June 2022 / Accepted: 13 July 2022 / Published online: 25 July 2022
© The Author(s), under exclusive licence to Springer Science+Business Media, LLC, part of Springer Nature 2022

Abstract

The interaction effect between collateral circulation and ischemic core size on stroke outcomes has been highlighted in acute ischemic stroke (AIS). However, biomarkers that assess the magnitude of this interaction are still lacking. We aimed to present a new imaging marker, the collateral-core ratio (CCR), to quantify the interaction effect between these factors and evaluate its ability to predict functional outcomes using machine learning (ML) in AIS. Patients with AIS caused by anterior circulation large vessel occlusion (LVO) were recruited from a prospective multicenter study. CCR was calculated as collateral perfusion volume/ischemic core volume. Functional outcomes were assessed using the modified Rankin Scale (mRS) at 90 days. An ML model was built and tested with a tenfold cross-validation using nine clinical and four imaging variables with mRS score 3–6 as unfavorable outcomes. Among 129 patients, CCR was identified as the most important variable. The prediction model incorporating clinical factors, ischemic core volume, collateral perfusion volume, and CCR showed better discriminatory power in predicting unfavorable outcomes than the model without CCR (mean C index 0.853 ± 0.108 versus 0.793 ± 0.133 , $P = 0.70$; mean net reclassification index $52.7\% \pm 32.7\%$, $P < 0.05$). When patients were divided into two groups based on their CCR value with a threshold of 0.73, unfavorable outcomes were significantly more prevalent in patients with $CCR \leq 0.73$ than in those with $CCR > 0.73$. CCR is a robust predictor of functional outcomes, as identified by ML, in patients with acute LVO. The prediction model that incorporated CCR improved the model's ability to identify unfavorable outcomes. ClinicalTrials.gov Identifier: NCT02580097.

Keywords Acute ischemic stroke · Large vessel occlusion · Collateral circulation · Prognosis · Machine learning

Abbreviations

AIS Acute ischemic stroke
CCR Collateral-core ratio
LVO Large vessel occlusion
mRS Modified Rankin Scale
ML Machine learning

Introduction

Growing evidence highlights the impact of collateral circulation on clinical outcomes in patients with large-vessel stroke [1–3]. The ischemic core is also likely to vary between

patients with respect to their collateral flow status. Clinical postulation states that acute ischemic stroke is proportional to the collateral circulation and inversely proportional to the ischemic core volume (clinical outcome measure = collateral circulation/ischemic core); this is well accepted, suggesting that an interaction effect between collateral circulation and ischemic core size may exist. Biomarkers that measure the magnitude of this interaction effect may provide valuable prognostic information on clinical outcomes. However, to date, no such biomarker has been reported.

Unlike quantitative hypoperfusion volume measurements, which are widely implemented in clinical trials using advanced software [4–6], collateral circulation is commonly assessed by semi-quantitative scores, and the volume of collateral flow cannot be routinely obtained. A recent study reported that the volume of perfusion from collateral flow (collateral perfusion volume) can be visualized and measured clinically using dual post-labeling delay (PLD) arterial spin

✉ Xin Lou
louxin@301hospital.com.cn

Extended author information available on the last page of the article

labeling (ASL) [7]. This approach processes the cerebral blood flow (CBF) at PLDs of 1500 ms and 2500 ms; thus, the late-arriving collateral inflow in the target downstream territory can be captured. It has been demonstrated that the collateral perfusion volume is associated with ischemic events in patients with middle cerebral artery stenosis. By utilizing this technology, it is possible to determine the relationship between the collateral perfusion volume and ischemic core volume. Additionally, the implementation of machine learning (ML) techniques, which are being increasingly applied in solving medical prediction tasks [8–10], allows for better feature selection and improves the accuracy of model construction.

Herein, we propose a new imaging marker, the collateral-core ratio (CCR), to quantify the magnitude of the interaction effect between collateral and ischemic core volumes. This study aimed to evaluate the ability of CCR to predict functional outcomes in patients with acute ischemic large vessel occlusive stroke using ML.

Methods

Study Design

The MR-based stroke mechanism and future risk score (MR-STARS) was a prospective multicenter observational study that recruited patients from 15 centers in China. Enrollment took place between January 1, 2019, and December 31, 2020. The study was approved by the institutional review boards of the participating institutions and registered at ClinicalTrials.gov (NCT02580097). Written informed consent was obtained from all the patients.

Patients

The inclusion criteria were as follows: (1) age > 18 years, (2) acute ischemic stroke caused by distal internal carotid artery or middle cerebral artery M1-M3 segment occlusion, (3) time from last known time of wellness to symptom onset within 24 h, (4) pre-stroke modified Rankin Scale (mRS) score 0–2, (5) availability of written informed consent, and (6) sufficient imaging quality for post-processing and review. The exclusion criteria were as follows: (1) other serious, advanced, or terminal illnesses or life expectancy < 3 months; (2) pregnancy; (3) time from last known time of wellness to symptom onset of > 24 h; (4) old lesions greater than 1/3 downstream territory or pre-stroke mRS score > 2; (5) loss to follow-up; and (6) insufficient imaging quality. The patient selection flowchart is shown in Fig. 1.

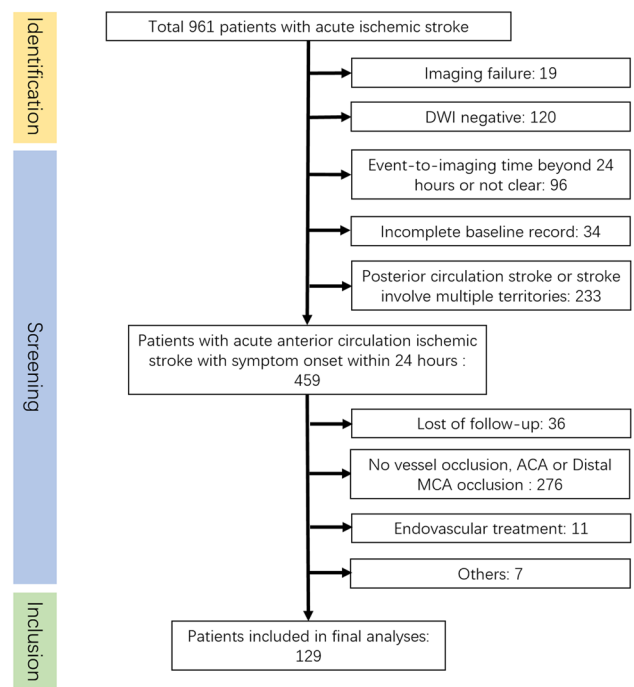


Fig. 1 Patient selection flowchart. Flowchart of patient selection and exclusion criteria in this study. Others include old, large lesions that are greater than 1/3 of the middle cerebral artery territory, multiple infarctions involving multiple territories, and death due to cancer

MRI Protocol

All MR studies were performed soon after patient arrival at the centers using a 3.0 T scanner (Discovery 750, GE Healthcare, Milwaukee, WI, USA) with a 32/8 channel head coil by a technician in the Department of Radiology without blinding. The MR protocol was as follows: T2-weighted imaging (WI), T1WI, T2 fluid-attenuated inversion recovery, diffusion-weighted imaging (DWI), MR angiography, three-dimensional pseudo-continuous arterial spin labeling (pCASL), and susceptibility-weighted imaging.

The pCASL protocol was as follows: repetition time = 4590 ms (PLD = 1500 ms), 5285 ms (PLD = 2500 ms), labeling duration = 1500 ms, echo time = 10.5 ms, field of view = 24 cm, 512 sampling points on eight spirals, spatial resolution = 3.64 mm, slice thickness = 4.0 mm, and number of slices = 36, with suppression of background. Images were acquired within 15 min.

Imaging Post-processing and Analysis

The ischemic core was measured using a commercially available software (NeuBrainCARE, Neurosoft) based on

DWI and apparent diffusion coefficient (ADC) maps as regions of $ADC < 620 \times 10^{-6} \text{ mm}^2/\text{s}$. Occasionally, manual delineation was performed when the software output was labelled incorrectly.

ASL CBFs were post-processed using the following steps: skull stripping, co-registration, and spatial normalization to the MNI (Montreal Neurological Institute) space coordinates. The figure of post-processing flow and further details are provided in the supplemental material. The hypoperfusion volumes on the 1500 ms and 2500 ms CBF were segmented by seed generation. The volume of collateral perfusion was obtained by segmentation of the residual signal on a 2 PLD CBF subtraction map using an in-house developed computer-aided software. Segmentation was performed using a regional growth method and then corrected by two neuroradiologists with > 10 years of experience. Based on the signal intensity distributions of the two PLD CBF subtraction maps, the seeds of the regional growth method were selected as the pixels on the affected side of the brain that had a signal intensity higher than the other 95% of pixels on the unaffected side of the territory. Additionally, the tolerance of the regional growth method was set to 2% of the maximum value of the two PLD CBF subtraction map. The quantitative CCR was calculated as follows: volume of collateral perfusion/volume of the ischemic core. The workflow was completed within 180 s for each case.

Treatment

The best medical therapies, including thrombolysis and conservative medical therapy for acute ischemic stroke, were provided in accordance with clinical guidelines [11].

Variables

We considered 13 baseline clinical factors, including age, sex, initial National Institutes of Health Stroke Scale (NIHSS) score, event-to-imaging time, risk factors (hypertension, diabetes, lipid disorders, coronary heart disease, and smoking), and baseline imaging parameters, including the affected vessel, ischemic core volume on DWI, collateral perfusion volume, and CCR. The complete list is presented in Table 1.

Outcome Measures

The primary study outcome measure was disability at 90 days, assessed using the mRS, with scores ranging from 0 (no symptoms) to 6 (death). Patients were followed up by phone call or outpatient consultation to evaluate the mRS score and record medication usage by neurologists or neuroradiologists who were blinded to the baseline clinical and imaging information. A favorable functional outcome was

Table 1 Patient demographics and comparison of patients with favorable and unfavorable clinical outcome

Features	Total	mRS > 2	mRS ≤ 2	P
Patients, n	129	53	76	
Age, years	64.05 ± 12.01	64.55 ± 11.52	63.71 ± 12.40	0.70
Sex				0.43
Male, n (%)	83	32 (60.4)	51 (67.1)	
Female, n (%)	46	21 (39.6)	25 (32.9)	
NIHSS, median (IQR)	8 (4–11)	10 (6–14)	4 (2.5–9)	< 0.001
Time from symptom onset to MRI	11.11 ± 7.82	10.92 ± 7.31	11.24 ± 8.19	0.82
Risk factors				
Hypertension, n (%)	83	34 (64.2)	49 (64.5)	0.97
Lipid disorders, n (%)	36	11 (20.8)	25 (32.9)	0.13
Diabetes, n (%)	42	17 (32.1)	25 (32.9)	0.92
Coronary heart disease, n (%)	25	7 (13.2)	18 (23.7)	0.14
Smoking, n (%)	54	25 (47.2)	29 (38.2)	0.31
Vessel affected				0.28
MCA, n (%)	101	39 (73.6)	62 (81.6)	
ICA, n (%)	28	14 (26.4)	14 (18.4)	
Imaging parameters				
Ischemic core volume, mL	33.08 ± 48.05	58.02 ± 60.01	15.69 ± 26.40	< 0.001
Collateral perfusion volume, mL	42.12 ± 40.39	29.24 ± 39.13	51.11 ± 39.03	< 0.001
Collateral-core ratio	2.07 (0.44–8.82)	0.43 (0.18–1.168)	4.61 (1.76–13.43)	< 0.001

NIHSS, National Institutes of Health Stroke Scale; MCA, middle cerebral artery; ICA, internal carotid artery

defined as mRS score 0–2; unfavorable functional outcome was defined as mRS score > 2.

Machine Learning Algorithms

To predict clinical outcomes using patient characteristics, the extreme gradient boosting (XGBoost) ML algorithm was trained for model construction [12]. XGBoost is a state-of-the-art ML algorithm under the gradient boosting framework. It provides parallel tree boosting for solving nonlinear classification problems in a highly efficient and accurate manner.

We used Shapley additive explanations (SHAP) to evaluate variable importance and interpret model predictions [13]. The SHAP is a powerful tool for explaining many types of ML. The magnitude of the SHAP values represents the contribution of the variable to prediction performance. A positive SHAP value indicates that the corresponding feature contributes to increasing the probability of the outcome, whereas a negative SHAP value suggests that the corresponding feature leads to a lower probability of the outcome [14].

A tenfold cross-validation policy was applied for model development and evaluation.

Statistical Analysis

Baseline characteristics were described and compared between the patients with favorable and unfavorable outcomes. Univariate comparisons were made using Pearson's χ^2 or Fisher's exact test for categorical variables and Student's *t*-test or Wilcoxon rank sum test for continuous variables, where appropriate.

Partial dependency plots suggest adjusted variable dependencies after integrating the effects of all other variables. The performance of the model was presented using Harrell's concordance index (C index), and the mean C index was compared using the *Z*-test in cross-validation. The net reclassification index (NRI) for measuring the model improvement in category discrimination was calculated to evaluate the model improvement of predictive ability by recruiting the CCR versus the traditional model. A higher NRI indicated better improvement. The CCR cutoff was identified in the receiver operating characteristic (ROC) curve by maximizing Yuden's *J* to discriminate patients with and without unfavorable outcomes. Based on the optimal CCR cutoff, the patients were stratified into high and low CCR groups. The XGBoost, Sklearn, and SHAP packages in Python were used in the analyses and plots. NRI was calculated using the "nricens" package in RStudio (Version 4.2.0) with a threshold of $P < 0.05$. All *P* values were two-sided, and statistical significance was set at $P < 0.05$.

Results

Patient Recruitment

Overall, 129 patients (83 men and 46 women; mean age, 64.05 ± 12.01 years) were included in the final analysis. Patients had a median NIHSS score of 8 (interquartile range (IQR) 4–11) and a mean time from symptom onset to MRI of 11.11 ± 7.82 h.

There were 101 cases of MCA occlusion involving the M1–M3 segments and 28 cases of ICA occlusion. The mean collateral perfusion volume was 42.12 ± 40.39 mL. The mean ischemic core volume was 33.08 ± 48.05 mL. The median CCR was 2.07 (IQR 0.44–8.82). The data distribution of the collateral perfusion volume, ischemic core volume, and their correlation are presented in Fig. 2A. The correlation matrix for all the continuous variables is shown in Fig. 2B. A total of 53 patients developed unfavorable clinical outcomes (90-day mRS score > 2), and 76 patients developed favorable clinical outcomes (90-day mRS score 0–2). The rate of unfavorable outcomes at 3 months was 41.1% (53/129) (Table 1).

Variable Importance in the ML Model

All the clinical and imaging parameters were entered into the XGBoost prediction model. The feature importance of all variables in the model was obtained in the form of SHAP values. Among them, CCR showed the highest feature importance, followed by NIHSS score (Fig. 3A, B). As the main objective was to investigate the incremental prognostic hierarchy of CCR, the top six important features, including CCR, ischemic core volume, collateral perfusion volume, and three clinical variables, were selected to train the model.

The associations between the top six important features (ranking from number 1 to 6: CCR, NIHSS, event-to-imaging time, age, collateral perfusion volume, and ischemic core volume) and the estimated probabilities of unfavorable outcomes at 3 months are presented by partial dependency plots in Fig. 3C. The estimated probability of unfavorable outcomes increased with increasing age, NIHSS score, event-to-imaging time, and ischemic core volume and a decrease in the collateral perfusion volume and CCR. A nonlinear association was observed between CCR and the probability of unfavorable outcomes.

Incremental Predictive Value of the CCR

After the XGBoost model was trained, tenfold cross-validation was performed to evaluate the model performance. The predictive model incorporating clinical factors, DWI

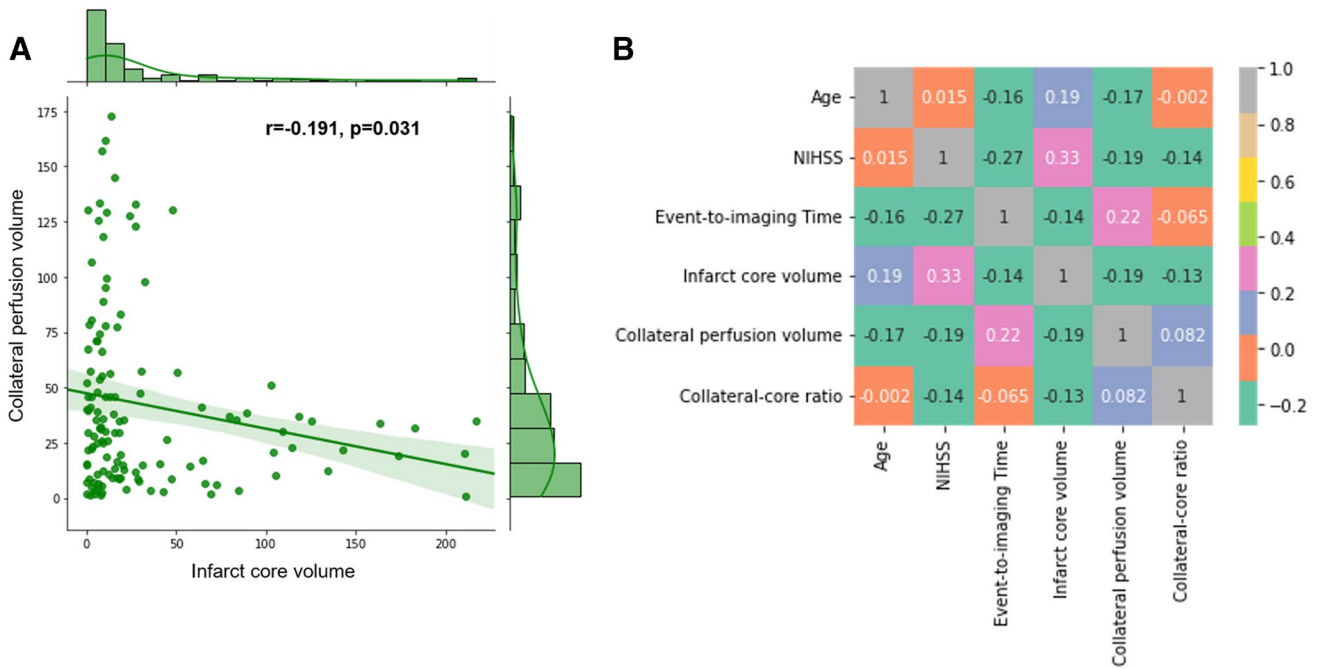


Fig. 2 Correlation analysis of variables. Scatter plot for all enrolled patients based on their collateral perfusion and infarct core volumes. Collateral perfusion volume showed a significant weak linear correla-

tion with the infarct core volume (A). Correlation matrix for all continuous variables (B)

ischemic core volume, collateral perfusion volume, and CCR showed better discriminatory power in predicting unfavorable outcomes than did the prediction model incorporating clinical factors, DWI ischemic core volume, and collateral perfusion volume (mean C index 0.853 ± 0.108 vs 0.793 ± 0.133 , $P = 0.70$; NRI 0.527 ± 0.327 , $P < 0.05$), as well as model including clinical factors and DWI ischemic core volume (mean C index 0.853 ± 0.108 vs 0.763 ± 0.114 , $P = 0.55$; NRI 0.565 ± 0.321 , $P < 0.05$) (Table 2).

Impact of CCR on Clinical Outcome

According to the ROC, the optimal CCR threshold was 0.73, with a sensitivity of 69.8%, specificity of 86.8%, and area under the curve of 0.832 for the prediction of 90-day mRS score > 2 (ROC curve is provided in Supplemental material). Forty-seven (36.4%) patients were classified as having a low CCR (≤ 0.73), and 82 (63.6%) patients had a high CCR (> 0.73).

A comparison of the clinical outcomes between the low and high CCR groups is listed in Table 3. Unfavorable outcomes were significantly more frequently observed in patients with low CCR than in those with high CCR (79.3% vs. 23.4%, $P < 0.001$). The 90-day mRS score distribution was significantly better in patients with high CCR than in those with low CCR (Fig. 4). One representative case is shown in Fig. 5 demonstrating an association between high

CCR and favorable clinical outcomes. Additional case is shown in Supplemental material.

Discussion

In the present study, by taking advantage of the quantitative measurement of collateral perfusion, the magnitude of the interaction effect between collateral flow and ischemic core was quantitatively analyzed. The proposed imaging marker, CCR, was the most important predictor of clinical outcomes. The accuracy of the prediction model incorporating clinical and imaging variables showed marked improvement after CCR recruitment.

Collateral circulation and ischemic core are critical pathophysiological parameters that determine neurological status [15, 16]. Although a linear correlation between the collateral circulation and ischemic core was presented [17], approximately 30% of patients with large infarct volumes had good collateral circulation and developed good clinical outcomes [18]. In contrast, approximately 15.4% of patients with small infarct volumes had poor collateral circulation and developed poor clinical outcomes [19, 20]. In addition, contrasting results regarding the association between collateral circulation and outcomes have been reported [21]. These findings suggest that the predictive power would be weakened by using collateral circulation or ischemic core

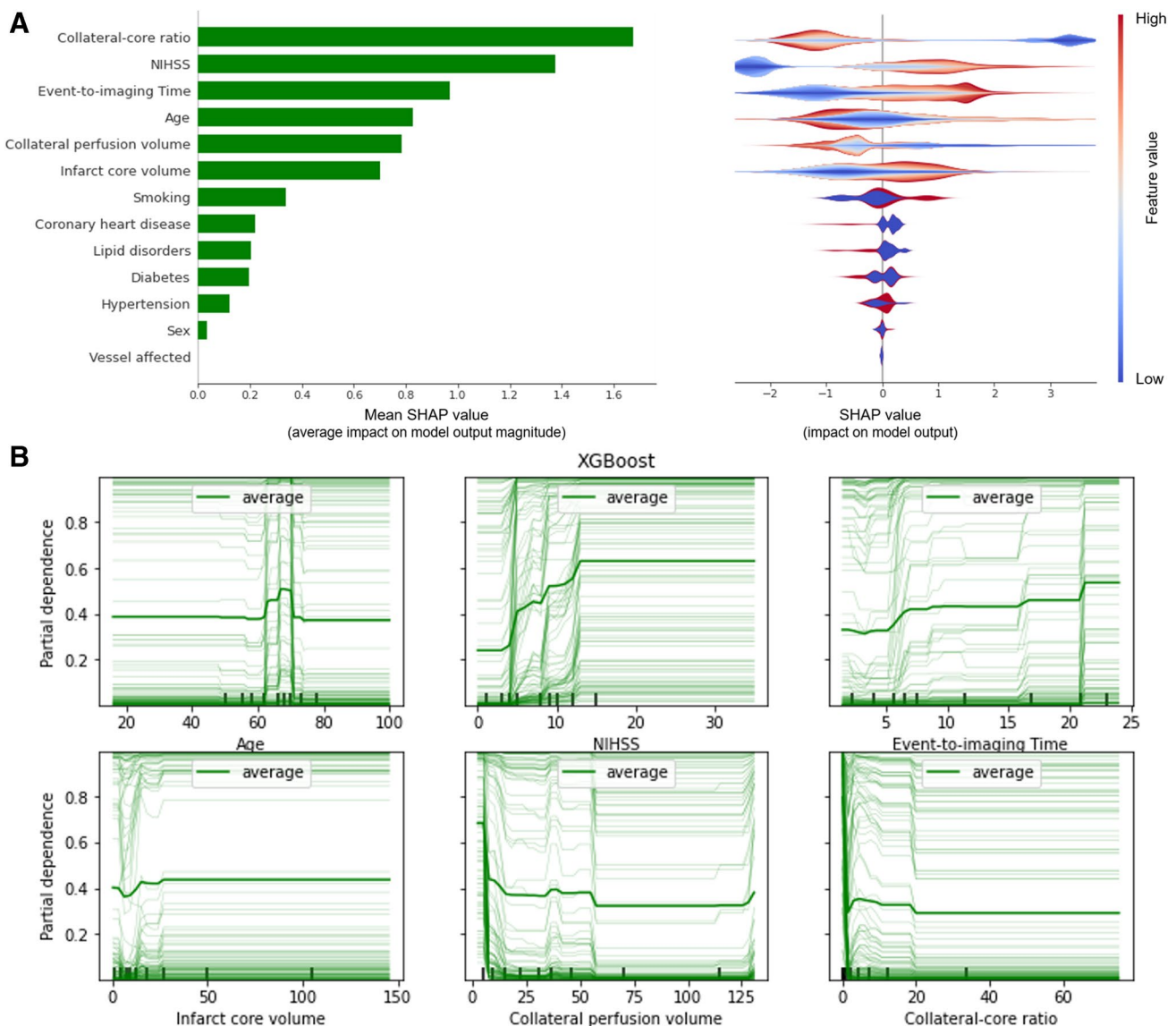


Fig. 3 Importance of variables and partial dependency plots. Left: Importance scores for variables included in the machine learning model to predict an unfavorable outcome as assessed by the Shapley additive explanations (SHAP) value. Variables with a higher SHAP value will have a greater impact on model performance. Right: Impact of individual variable on the model’s prediction. A positive SHAP value indicates that the corresponding feature contributes to an increase in the probability of an unfavorable outcome, whereas a negative SHAP value indicates that the corresponding feature leads

to a lower probability of an unfavorable outcome. Taking collateral-core ratio as an example, the lower the collateral-core ratio is, the greater the risk of an unfavorable outcome. The width of each variable reflects the frequency of case points (A). Partial dependency plots show the effect of the top six important features on clinical outcomes. While the middle thick line indicates the average effect of the selected variable, the thin lines indicate the effect of each case. The nonlinear association between the selected variables and stroke outcomes after adjustment of all other variables is illustrated (B)

volume alone, and the interaction effect between them may be highlighted.

Few studies have directly assessed the interaction between collateral circulation and infarct volume in acute large vessel occlusive stroke. In our study, the added value of CCR in predicting stroke outcomes, as identified by ML, demonstrated that the interaction information was valuable in the construction of the prediction model.

Our method defines the volume of collateral flow by the volume of tissue with a time-based arterial spin-labeled signal arrival beyond a threshold based on contralateral brain CBF. In essence, there is a methodology overlap with standard exogenous contrast analyses: penumbral tissue and hypoperfusion intensity ratio, typically defined by delayed contrast arrival metrics such as T_{\max} [6]. However, the CCR is conceptually different since the CCR investigates

Table 2 Performances and comparisons of the prediction models

XGBoost model	Mean C index (SD)	P value	Mean NRI (SD)	P value
Model 3 vs model 1	0.853 (0.108) vs 0.763 (0.114)	0.55	0.565 (0.321)	< 0.05
Model 3 vs model 2	0.853 (0.108) vs 0.793 (0.133)	0.70	0.527 (0.327)	< 0.05

Model 1: Clinical parameters (National Institutes of Health Stroke Scale, event-to-imaging time and age)+ ischemic core volume

Model 2: Clinical parameters + ischemic core volume + collateral perfusion volume

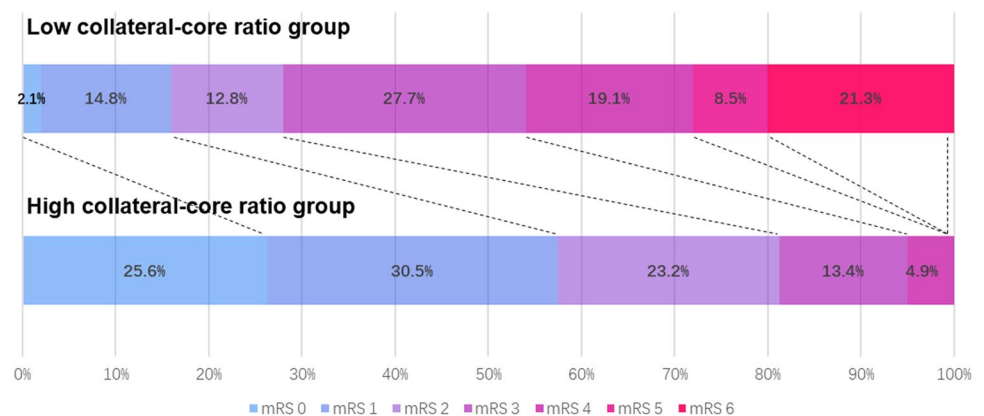
Model 3: Clinical parameters + ischemic core volume + collateral perfusion volume + collateral-core ratio

The performance of each prediction model based on XGBoost is assessed by the tenfold cross-validation. XGBoost, extreme gradient boosting; SD, standard deviation

Table 3 Comparison of clinical outcomes in the low and high collateral-core ratio groups

Factor	High collateral-core ratio	Low collateral-core ratio	P
N	82	47	
Favorable outcomes (mRS score 0–2), n (%)	65 (79.3)	11 (23.4)	<0.001
Excellent outcomes (mRS score 0–1), n (%)	46 (56.1)	5 (10.6)	<0.001
Moderate outcomes (mRS score 0–3), n (%)	76 (92.7)	24 (51.1)	<0.001

Fig. 4 Influence of collateral-core ratio on clinical outcomes. The comparison of the 90-day modified Rankin scale score distribution, which is significantly shifted to better functional independence in the high collateral-core ratio group



the interaction effect between collaterals and ischemic core rather than penumbral tissue, and the hypoperfusion intensity ratio is presented to define the status of collateral circulation [22]. Nevertheless, CCR may also be viewed for hypothesis generation and transplanted to multimodal CT because most centers use CT angiography and CT perfusion for acute stroke imaging.

Pial collateral status, which can be assessed by conventional angiography, single-phase or multiphase CT angiography [23], and perfusion imaging [24], commonly present as semi-quantitative grading scales. Dual-PLD ASL collateral assessment is a quantitative method that has been reported in a series of studies from different groups [7, 25, 26]. The measurement of collateral perfusion on subtraction images was conducted by manual segmentation previously; in the present study, we developed an in-house software to perform skull stripping, spatial co-registration, normalization, and automatic segmentation, which greatly reduced

noise-generation and improved the reliability of collateral perfusion measurement.

Because the imaging parameters are correlated with each other, feature collinearity might reduce the performance of linear models, such as logistic regression, while having little impact on the XGBoost model, which characterizes tree boosting. In addition, partial dependency plots showed a nonlinear relationship between many features and clinical outcomes; so the XGBoost ML algorithm rather than linear models was preferable in our study.

Our study has several clinical implications. First, the study demonstrated an interaction effect between collateral circulation and infarct volume on stroke outcomes and provided a cutoff value for interpreting the quantitative relationship in determining clinical outcomes in patients with acute large vessel stroke. Second, the marker was applicable to a more generalized population. In essence, although the time window and patient inclusion criteria have been

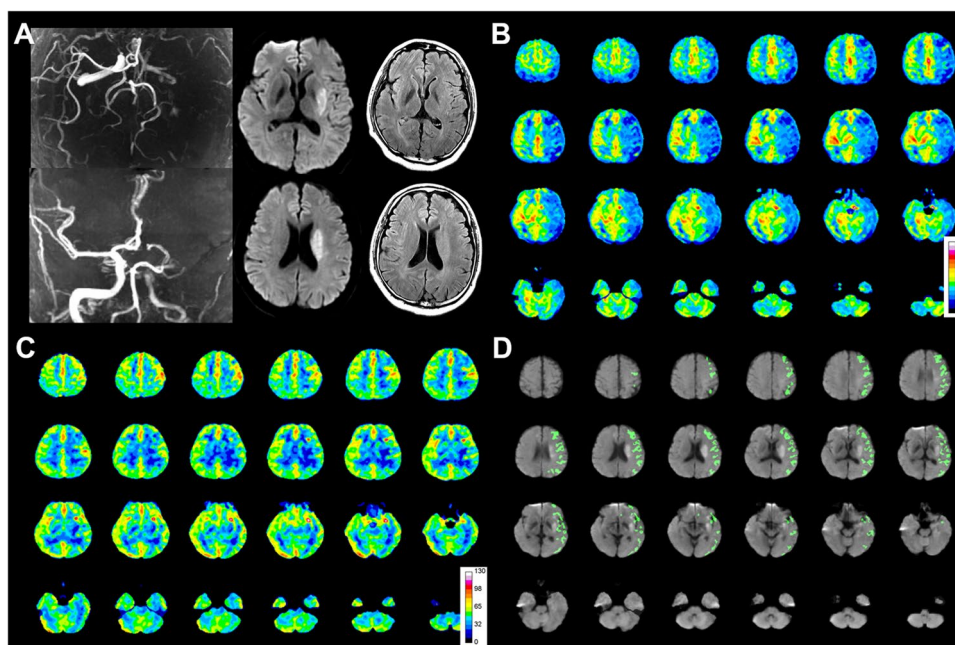


Fig. 5 Representative case exhibiting a high collateral-core ratio and a better clinical outcome. Figure shows a 40-year-old male patient with acute left distal internal carotid and middle cerebral artery occlusion. Diffusion-weighted imaging (DWI) demonstrates a basal ganglia region infarction with a volume of 12.65 mL (A). Territorial hypoperfusion can be observed on cerebral blood flow maps on

arterial spin labeling with a post-labeling delay (PLD) of 1500 ms (B). Delayed inflow in the territory is visible on cerebral blood flow maps from PLD of 1500 ms to 2500 ms (C). The volume of collateral perfusion as overlaid green mask on DWI is 45.74 mL (D). The collateral-core ratio is measured as 3.62. The patient achieved a good functional outcome (3-month mRS score is 1)

extended, only a small proportion of stroke patients can receive endovascular treatment (representing only 3.1% of patients in 2016 all over the USA) for many subjective reasons, including capacity of stroke centers, physician skill, and related resources [27]. Since penumbral imaging has been the standard assessment of patients considering endovascular treatment, imaging markers for treatment response in those considering the best medical treatment have not yet been developed. The proposed CCR provides an alternative biomarker for clinical outcome prediction and may help to support treatment. Third, ASL requires no contrast administration, which is applicable for elderly individuals or those with kidney disease and reduces the contrast burden during the entire course of diagnosis and treatment [28]. The post-processing flow is fast and requires no complicated steps, which means that the method is suitable for rapid assessment of patients prior to decisions.

This study had some limitations. First, the arrival of collateral flow may be further delayed due to large vessel occlusion, leading to the underestimation of collateral perfusion by the dual-PLD ASL method. The measured collateral perfusion may only be a part of the total collateral flow or the early arriving part of the collateral flow. However, this early arriving part of the collateral flow may be more important and in accordance with the rapid collateral flow, as assessed by digital subtraction angiography or CT

angiography, serving as a highly efficient compensated flow to the ischemic territory. Second, the relatively long scanning time of the study protocol and some technical concerns, for example, the different implementations of ASL (pulsed ASL versus pCASL) and signal loss with lower field strength scanners (making 3 T a minimum technical requirement), should be considered during clinical practice. Third, the small size of the cohort imposed limitations on the accuracy of the ML model and statistical modeling in general. And, these results only pertain to acute stroke patients with moderate or mild stroke who had an occlusion visible on vascular imaging and received the best medical therapy.

Conclusions

CCR as the top predictor of functional independence at 90 days was identified by ML in patients with stroke due to acute anterior large vessel occlusion. This new imaging marker provides a quantitative assessment of the magnitude of the physiological interaction effect between the collateral circulation and ischemic core size. The prediction model that included CCR, along with clinical and imaging parameters, showed remarkably improved predictive performance. Further studies employing standard exogenous contrast methods are required to validate these findings.

Supplementary Information The online version contains supplementary material available at <https://doi.org/10.1007/s12975-022-01066-9>.

Author Contribution Author contributions are as follows: X. L. and X. Z. conceived and designed the study. J. H. L., Z. H. M., X. Y. W., W. C., G. H. W., Q. L. N., X. L., Y. T. B., D. H., W. T. G., S. Y., X. B. B., Y. N. L., L. X. W., S. H. Z., T. Y. Z., Q. D., and C. H. D. acquired and analyzed the data. J. H. L., S. X., and X. L. drafted the manuscript. L. C., C. L. T., X. Z., and X. L. revised the manuscript.

Funding This work was supported by the National Natural Science Foundation of China (Nos. 81825012, 81730048, and 82151309 to X. L.; Nos. 81625011 and 21921004 to X. Z.; and No. 81901708 to J. H. L.).

Data Availability Statement The data that support the findings of this study are available on request from the corresponding author. The data are not publicly available due to privacy or ethical restrictions.

Declarations

Ethics Approval The study was approved by the ethics committee of Chinese PLA General Hospital (S2018-193–01). This study was performed in line with the principles of the Declaration of Helsinki.

Informed Consent Informed consent was obtained from all individual participants included in the study.

Conflict of Interest The authors declare no competing interests.

References

- Albers GW, Goyal M, Jahan R, et al. Ischemic core and hypoperfusion volumes predict infarct size in SWIFT PRIME. *Ann Neurol*. 2016;79:76–89.
- Bang OY, Goyal M, Liebeskind DS. Collateral circulation in ischemic stroke: assessment tools and therapeutic strategies. *Stroke*. 2015;46:3302–9.
- Goyal M, Menon BK, van Zwam WH, et al. Endovascular thrombectomy after large-vessel ischaemic stroke: a meta-analysis of individual patient data from five randomised trials. *Lancet*. 2016;387:1723–31.
- Goyal M, Demchuk AM, Menon BK, et al. Randomized assessment of rapid endovascular treatment of ischemic stroke. *N Engl J Med*. 2015;372:1019–30.
- Jovin TG, Chamorro A, Cobo E, et al. Thrombectomy within 8 hours after symptom onset in ischemic stroke. *N Engl J Med*. 2015;372:2296–306.
- Albers GW, Marks MP, Kemp S, et al. Thrombectomy for stroke at 6 to 16 hours with selection by perfusion imaging. *N Engl J Med*. 2018;378:708–18.
- Lou X, Ma X, Liebeskind DS, et al. Collateral perfusion using arterial spin labeling in symptomatic versus asymptomatic middle cerebral artery stenosis. *J Cereb Blood Flow Metab*. 2019;39:108–17.
- Xue B, Li D, Lu C, et al. Use of machine learning to develop and evaluate models using preoperative and intraoperative data to identify risks of postoperative complications. *JAMA Netw Open*. 2021;4:1–14.
- Khera R, Haimovich J, Hurley NC, et al. Use of machine learning models to predict death after acute myocardial infarction. *JAMA Cardiol*. 2021;6:633.
- Sirsat MS, Fermé E, Câmara J. Machine learning for brain stroke: a review. *J Stroke Cerebrovasc Dis*. 2020;29: 105162.
- Powers WJ, Rabinstein AA, Ackerson T, et al. 2018 guidelines for the early management of patients with acute ischemic stroke: a guideline for healthcare professionals from the American Heart Association/American Stroke Association. *Stroke*. 2018;49:e46–110.
- Chen T, Guestrin C. XGBoost: a scalable tree boosting system. *Proc ACM SIGKDD Int Conf Knowl Discov Data Min*. 2016;13–17:785–94.
- Lundberg SM, Erion G, Chen H, et al. From local explanations to global understanding with explainable AI for trees. *Nat Mach Intell*. 2020;2:56–67.
- Lundberg SM, Nair B, Vavilala MS, et al. Explainable machine-learning predictions for the prevention of hypoxaemia during surgery. *Nat Biomed Eng*. 2018;2:749–60.
- Chen C-J, Ding D, Starke RM, et al. Endovascular vs medical management of acute ischemic stroke. *Neurology*. 2015;85:1980–90.
- Rodrigues FB, Neves JB, Caldeira D, et al. Endovascular treatment versus medical care alone for ischaemic stroke: systematic review and meta-analysis. *BMJ*. 2016;i1754.
- Rusanen H, Saarinen JT, Sillanpää N. Collateral circulation predicts the size of the infarct core and the proportion of salvageable penumbra in hyperacute ischemic stroke patients treated with intravenous thrombolysis. *Cerebrovasc Dis*. 2015;40:182–90.
- Broocks G, Knierp H, Schramm P, et al. Patients with low Alberta Stroke Program Early CT Score (ASPECTS) but good collaterals benefit from endovascular recanalization. *J Neurointerv Surg*. 2020;12:747–52.
- Yu I, Bang OY, Chung JW, et al. Admission diffusion-weighted imaging lesion volume in patients with large vessel occlusion stroke and Alberta Stroke Program Early CT Score of ≥ 6 points: serial computed tomography-magnetic resonance imaging collateral measurements. *Stroke*. 2019;50:3115–20.
- Bivard A, Lou M, Levi CR, et al. Too good to treat? Ischemic stroke patients with small computed tomography perfusion lesions may not benefit from thrombolysis. *Ann Neurol*. 2016;80:286–93.
- De Havenon A, Mlynash M, Kim-Tenser MA, et al. Results from DEFUSE 3: good collaterals are associated with reduced ischemic core growth but not neurologic outcome. *Stroke*. 2019;50:632–8.
- Olivot JM, Mlynash M, Inoue M, et al. Hypoperfusion intensity ratio predicts infarct progression and functional outcome in the DEFUSE 2 cohort. *Stroke*. 2014;45:1018–23.
- Menon BK, D’Este CD, Qazi EM, et al. Multiphase CT angiography: a new tool for the imaging triage of patients with acute ischemic stroke. *Radiology*. 2015;275:510–20.
- Kim SJ, Son JP, Ryoo S, et al. A novel magnetic resonance imaging approach to collateral flow imaging in ischemic stroke. *Ann Neurol*. 2014;76:356–69.
- Lyu J, Ma N, Liebeskind DS, et al. Arterial spin labeling magnetic resonance imaging estimation of antegrade and collateral flow in unilateral middle cerebral artery stenosis. *Stroke*. 2016;47:428–33.
- Lyu J, Ma N, Tian C, et al. Perfusion and plaque evaluation to predict recurrent stroke in symptomatic middle cerebral artery stenosis. *Stroke Vasc Neurol*. 2019;4:129–34.
- MacKenzie IER, Moeini-Naghani I, Sigounas D. Trends in endovascular mechanical thrombectomy in treatment of acute ischemic stroke in the United States. *World Neurosurg*. 2020;138:e839–46.
- Alsop DC, Detre JA, Golay X, et al. Recommended implementation of arterial spin-labeled perfusion MRI for clinical applications: a consensus of the ISMRM perfusion study group and the European consortium for ASL in dementia. *Magn Reson Med*. 2015;73:102–16.

Publisher's Note Springer Nature remains neutral with regard to jurisdictional claims in published maps and institutional affiliations.

Springer Nature or its licensor holds exclusive rights to this article under a publishing agreement with the author(s) or other rightsholder(s); author self-archiving of the accepted manuscript version of this article is solely governed by the terms of such publishing agreement and applicable law.

Authors and Affiliations

Jinhao Lyu¹ · Sa Xiao^{2,3} · Zhihua Meng⁴ · Xiaoyan Wu⁵ · Wen Chen⁶ · Guohua Wang⁷ · Qingliang Niu⁸ · Xin Li⁹ · Yitong Bian¹⁰ · Dan Han¹¹ · Weiting Guo¹² · Shuai Yang¹³ · Xiangbing Bian¹ · Qi Duan¹ · Yina Lan¹ · Liuxian Wang¹ · Tingyang Zhang¹ · Caohui Duan¹ · Ling Chen¹⁴ · Chenglin Tian¹⁵ · Yuesong Pan^{16,17} · Xin Zhou² · Xin Lou¹  · on behalf of the MR-STARS Investigators

¹ Department of Radiology, Chinese PLA General Hospital/Chinese PLA Medical School, 28 Fuxing Road, Beijing 100853, China

² Key Laboratory of Magnetic Resonance in Biological Systems, State Key Laboratory of Magnetic Resonance and Atomic and Molecular Physics, National Center for Magnetic Resonance in Wuhan, Wuhan Institute of Physics and Mathematics, Innovation Academy for Precision Measurement Science and Technology, Chinese Academy of Sciences-Wuhan National Laboratory for Optoelectronics, Wuhan, China

³ University of Chinese Academy of Sciences, Beijing, China

⁴ Department of Radiology, Yuebei People's Hospital, Guangdong, China

⁵ Department of Radiology, Anshan Changda Hospital, Liaoning, China

⁶ Department of Radiology, Shiyan Taihe Hospital, Hubei, China

⁷ Department of Radiology, Qingdao Municipal Hospital Affiliated to Qingdao, University, Qingdao, China

⁸ Department of Radiology, WeiFang Traditional Chinese Hospital, Shandong, China

⁹ Department of Radiology, The Second Hospital of Jilin University, Jilin, China

¹⁰ Department of Radiology, The First Affiliated Hospital of Xi'an Jiaotong University, Shaanxi, China

¹¹ Department of Radiology, the First Affiliated Hospital of Kunming Medical University, Yunnan, China

¹² Department of Radiology, Shanxi Provincial People's Hospital, Shanxi, China

¹³ Department of Radiology, Xiangya Hospital Central South University, Hunan, China

¹⁴ Department of Neurosurgery, Chinese PLA General Hospital, Beijing, China

¹⁵ Department of Neurology, Chinese PLA General Hospital, Beijing, China

¹⁶ China National Clinical Research Center for Neurological Diseases, Beijing Tiantan Hospital, Capital Medical University, Beijing, China

¹⁷ Department of Neurology, Beijing Tiantan Hospital, Capital Medical University, Beijing, China